INTECH
open science | open minds

OPEN ACCESS
ARTICLE

Nanomaterials and Nanotechnology

A Facile Synthesis of Pt Nanoflowers Composed of an Ordered Array of Nanoparticles

Invited Article

Anirban Dandapat[1], Anuradha Mitra[1], Prateek K. Gautam[1,2] and Goutam De[1,*]

1 Nano-Structured Materials Division, CSIR-Central Glass and Ceramic Research Institute, Kolkata, India
2 Summer student from Department of Chemical Engineering at IIT-Guwahati, India
* Corresponding author E-mail: gde@cgcri.res.in

Received 4 April 2013; Accepted 5 July 2013

© 2013 Dandapat et al.; licensee InTech. This is an open access article distributed under the terms of the Creative Commons Attribution License (http://creativecommons.org/licenses/by/3.0), which permits unrestricted use, distribution, and reproduction in any medium, provided the original work is properly cited.

Abstract Platinum nanoflowers (Pt NFs) composed of an ordered assembly of nanoparticles were synthesized by an ethanol reduction of $[PtCl_6]^{2-}$ under a reflux condition (85 °C) at pH 2.5 in the presence of PVP (molecular weight 10,000) as a structure-directing agent. Optical and transmission electron microscopic (TEM) studies confirmed the reduction of $[PtCl_6]^{2-}$ into Pt^0 followed by its growth to form Pt NPs of a size of ~4 nm, which were then assembled into ordered NFs through epitaxial growth along the (111) plane. The mechanism of the Pt NFs' formation with respect to the use of PVP of different molecular weights and the pH of the reaction is discussed in detail.

Keywords Pt Nanoflower, Synthesis, PVP, Ethanol Reduction

1. Introduction

Platinum nanoparticles (Pt NPs) have attracted significant attention owing to their unique physical and chemical properties. The use of Pt NPs as a catalyst is very popular due to its implication in the production of hydrogen gas from cyclohexane [1], the reduction of pollutant gases from car exhausts [2], their application in direct methanol fuel cells (DMFCs) [3] and other important reactions [4-6]. The properties of the NPs are largely dependent upon their size, shape and morphology. This triggered an intense amount research to develop various shaped Pt NPs [7-9]. NPs with a complex structure and a tuneable size and morphology have been a focus of attention because such control is crucial for the determination of many structure-property relationships. Recently, porous, flowerlike Pt NPs have been shown to possess superior catalytic activity [10-15] because of their high surface area, roughness and exposure to certain high index facets towards a specific reaction with enough adsorption sites for all involved molecules in a narrow space. Therefore, our interest revolves around the synthesis of flower-shaped Pt NPs, which could be very much useful in the field of catalysis and related applications.

Recently, many research groups have been involved in the synthesis of flower-like Pt NPs via several methods, viz. the liquid crystal approach [16], the hard-templating

approach [17] and the solution-based method [18-22]. The most common processes involve solution phase chemical reactions, which enable the large scale synthesis of NPs with a controllable size and shape. While Xia et al. [18] used an iron-mediated polyol process to synthesize hierarchically structured, flower-like Pt nano agglomerates, Ren and Tilley [19] reported the synthesis of multi-branched nanopolypods of Pt through the reduction of platinum acetylacetonate in toluene under pressure from hydrogen in the presence of oleylamine as a surfactant. Sun et al. [20] reported template- and surfactant-free self-assembles of 3D Pt NFs via the chemical reduction of hexachloroplatinic acid with formic acid. Kawasaki et al. [21] used a galvanic replacement reaction to synthesize Pt NFs. Yin et al. [22] described the iodine ion-mediated formation of Pt NFs. Yamauchi et al. [16,17,23] reported some Pt-containing nanoporus flower-shaped particles as displaying very high electrocatalytic activities. There are also a few reports where Pt NFs were synthesized on a carbon support [24,25], with the resultant composite exhibiting enhanced catalytic and sensing abilities due to the unique morphology of the flower-shaped particles. In a very recent study, Mohanty et al. [10] adopted a new approach to synthesize ordered Pt NFs using a laboratory-synthesized amino acid-based surfactant and ascorbic acid as a reducing agent.

The synthesis of such NFs involves controlled assemblies and the epitaxial growth of individual NPs rather than the formation of random aggregates, which is extremely hard to control. This motivated us to synthesize ordered Pt NFs using an economically cheap and easily available stabilizing agent PVP. In this manuscript, apart from a detailed investigation on the effect of pH as well as the role of PVP in the formation mechanism of Pt NFs, we demonstrate a facile and efficient route for the large scale synthesis of flower-like platinum nanostructures composed of small Pt NPs grown epitaxially in an ordered fashion via the ethanol reduction of H_2PtCl_6 at 85±1 °C in the presence of low molecular weight PVP-10 (MW 10,000).

Numerous studies reported so far involve the synthesis of Pt NPs via the alcohol reduction process in the presence of PVP [26,27]. It is well known that the oxygen atoms of the carbonyl groups and the nitrogen atoms of PVP interact with the surface of the metal NP to stabilize the NPs [28,29]. The main goal of these works was to synthesize very small NPs (~2–5 nm). For this purpose, a PVP with a relatively high molecular weight (MW) and a nearly neutral pH was used [26,27]. In an acidic medium, PVP remains in a cationic form and the O atoms of the carbonyl group become weakly bonded with H^+ ions of the medium. Therefore, the interaction between the O atoms and the metal surface becomes labile, resulting in the growth of the particle to a relatively larger size. It is also to be noted that a PVP with higher MW binds the NPs more strongly than its low MW analogue, and thus a higher MW PVP restricts the further growth of the NPs [30]. For this reason, we have chosen a low MW PVP for the three-dimensional growth of the Pt NPs.

2. Experimental Section

2.1 Materials

Hexachloroplatinic acid (H_2PtCl_6) and a series of polyvinylpyrrolidone sold as PVP-10, PVP-40 and PVP-1300 (MW 10,000, 40,000 and 1300,000 respectively) were obtained from Sigma Aldrich. Absolute ethanol (99.99%) and hydrochloric acid were purchased from Merck and Rankem Chemicals respectively. Milli-Q water (resistivity, 18.2 MΩ.cm), obtained from the Millipore water purification system, was used for all purposes. All glass wares were thoroughly cleaned with aqua regia, rinsed with Milli-Q water and dried in air before use. All chemicals were used as received without further purification.

2.2 Preparation of the Pt NFs

The molar ratio of platinum and PVP was maintained at 1:20 for the synthetic process using ethanol as the reducing agent. 25 ml of 2.0 mM H_2PtCl_6 (0.05 mmol) solution was taken in a 250 ml round bottom flask. 0.112 g (1.0 mmol) of solid PVP-10 was dissolved in 1 ml ethanol and added to the above solution. Furthermore, a calculated amount of 1M HCl was added to adjust the pH of the final solution, which was diluted with 35 ml water. This reaction mixture was put on an electric heating mantle with refluxing apparatus. As soon as refluxing began, 22.5 ml of absolute ethanol was added to the reaction flask. The mixture was then allowed to reflux and fitted with a condenser. The temperature inside the boiling fluid was 85±1 °C, measured using a thermometer. An appearance of a dark black-brown colour was observed after around 30 min. The reflux was continued up to 12 h. At different time intervals, some aliquot of the solution was collected during the refluxing for characterization.

2.3 Characterization of the Pt NFs

The reduction of Pt^{IV} (H_2PtCl_6) → Pt^0 was followed by taking out samples from the reaction mixture at every 10 min interval, followed by diluting it 5 times and then studying the attrition of the strong absorbance band for the $[PtCl_6]^{2-}$ ions by a UV-visible spectrometer. For the GIXRD studies, the Pt NFs' solution (formed after refluxing for 6 h) was drop-cast on a microscope glass slide and dried in an oven at 60 °C. Thereafter, XRD data was recorded by a Rigaku SmartLab operating at 9 kW

(using Cu Kα radiation, λ=1.54059 Å) with a grazing incidence angle of 1°. Samples for transmission electron microscope (TEM) were prepared by evaporating the solvent from the few drops of Pt NFs solution cast on a carbon-coated Cu grid. Tecnai G² 30ST (FEI), operating at 300 kV, was used to obtain the TEM micrographs for the Pt NFs. High resolution TEM (HRTEM) and selected area electron diffraction (SAED) patterns were obtained using the resources attached with the TEM.

3. Results and Discussion

The formation of PVP-10 stabilized Pt NPs via the ethanol reduction of Pt^{IV} to Pt^0 was monitored by UV-visible spectroscopy where the absorbance peak of $[PtCl_6]^{2-}$ ions at different time intervals were recorded as shown in Figure 1. The intensity of the absorbance peak at ~255 nm, characterizing a ligand-to-metal charge transfer (LMCT) [26] band of a $[PtCl_6]^{2-}$ complex decreased gradually and disappeared after 30 min, confirming the completion of the reduction process. The gradual shifting of the baseline to a higher value indicates an increase in the overall absorbance of the solution. The reaction mixture turned black via a dark brownish hue. This hints at more nucleation and also at the beginning of the association of the NPs into a bigger size. It is to be noted that an initial shifting of the absorbance peak of $[PtCl_6]^{2-}$ ions in the absence (inset of Figure 1) and in the presence of the PVP from ~263 to ~255 nm, respectively, confirms the interaction between the Pt ions and the PVP [26]. Several research groups reported that highly stable Pt NPs in the size range of 2–7 nm can be synthesized using the PVP with MW 40,000–1,300,000 without using any additional acids [26,27]. As described previously, the interaction between the PVP and metal becomes labile in the case of relatively low MW PVP under acidic pH. Therefore, we observed the growth of the NPs using a low MW PVP (PVP-10) at pH ~5 (Figure 2a). A further decrease in pH led to the formation of the assembled growth of particles in the presence of PVP-10 (Figure 2b). A controlled experiment with a very high MW (MW=1,300,000; PVP-1300) PVP under similar reaction conditions did not show any flower-like growth (Figure 2c,d). However, some growth of particles with PVP-40 (MW 40,000) at pH ~2.5 was observed. Clearly, at a low pH (~2.5), the NF-shaped particles were formed when PVP-10 was used as a stabilizing agent (Figure 2b). Thus, detailed studies of these NFs were carried out and described in the following sections.

During the refluxing conditions, ethanol mainly serves as the reducing agent in the conversion of Pt^{IV} to Pt^0, while PVP polymeric chains impart a protective capping on the surface of the NPs. However, PVP also has a reducing property (relatively weaker than ethanol) that might help the reduction procedure [32,33]. In the process, ethanol releases nascent hydrogen and is oxidized to an aldehyde (Eq. 1). H_2PtCl_6 is converted to $PtCl_4$ according to Eq. 2 and is subsequently reduced by the nascent hydrogen (released by alcohol) to form Pt metal (Pt^0), as shown in Eq. 3. The reflux was continued up to 12 h.

$$CH_3CH_2OH \rightarrow CH_3CHO + [H] \quad (1)$$

$$H_2PtCl_6 \rightarrow 2HCl + PtCl_4 \quad (2)$$

$$PtCl_4 + 4H \rightarrow Pt^0 + 4HCl \quad (3)$$

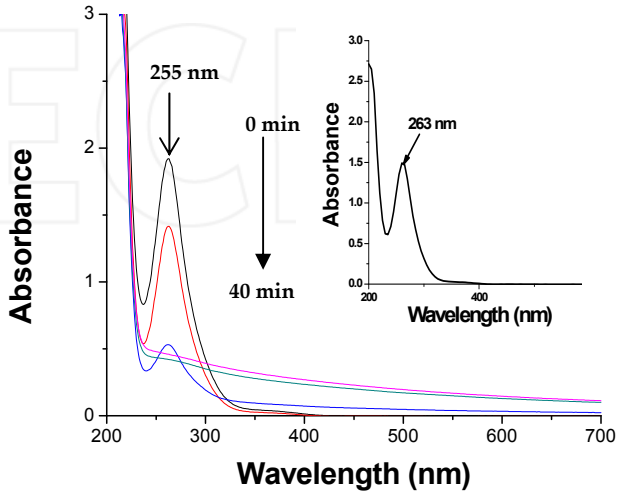

Figure 1. UV-visible absorption spectra obtained at different times of refluxing during the reduction of Pt^{IV} (H_2PtCl_6) to Pt^0 in PVP-10. The absorption spectrum of the H_2PtCl_6 solution without any PVP is shown in the inset.

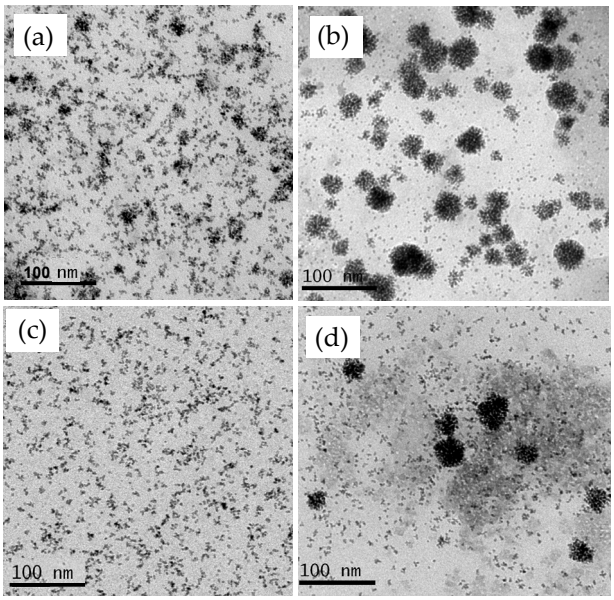

Figure 2. TEM micrographs of Pt NPs synthesized via refluxing at 85 °C for 3 h using: (a) PVP-10 at pH 5, (b) PVP-10 at pH 2.5, (c) PVP-1300 at pH 2.5 and (d) PVP 40 at pH 2.5.

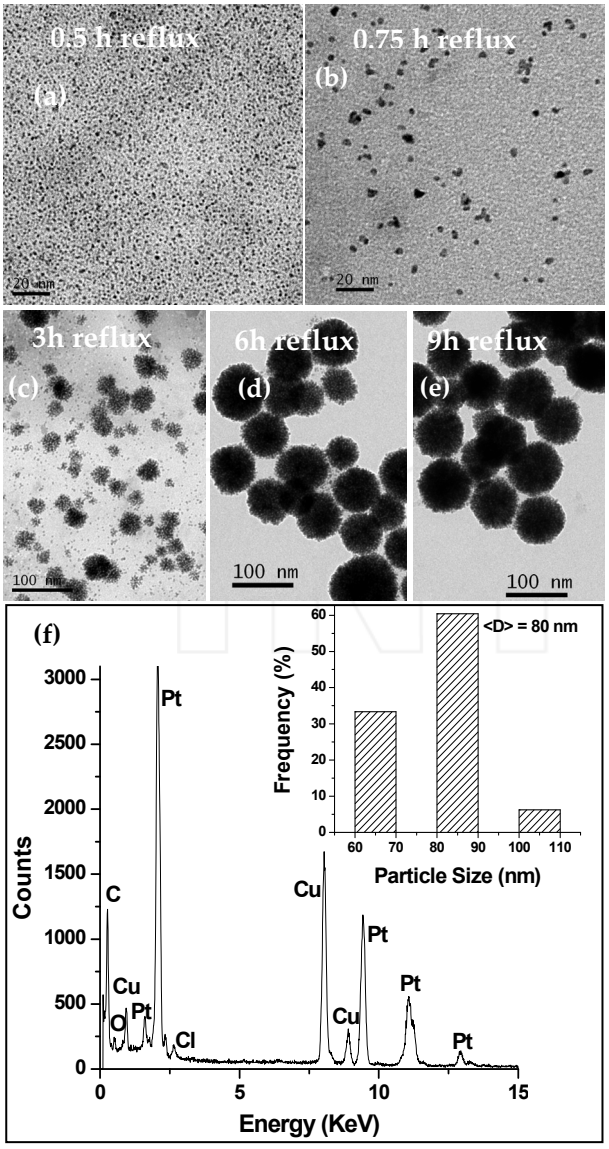

Figure 3. TEM studies of Pt NPs solution obtained after refluxing at: (a) 0.5 h, (b) 0.75 h (c) 3 h, (d) 6 h and (e) 9 h. (f) The EDX pattern and the histogram of the particles (inset) were obtained from a 6 h refluxed sample.

To understand the growth phenomena, TEM images of Pt NPs were taken from the solutions at different time intervals after refluxing for 0.5, 0.75, 3.0, 6.0 and 9.0 h. After 0.5 h of refluxing, the TEM micrograph shows the formation of very small NPs (Figure 3a). These small NPs (~1–2 nm) grew rapidly to ~3–5 nm upon further refluxing (0.75 h; Figure 3b). The change could be perceived by the change in solution colour from colourless to brown. The TEM image of the 3 h refluxed Pt solution showed structures similar to flowers (Pt NFs) within the size range of 20–50 nm (Figure 3c), along with smaller particles. However, the 6 h and 9 h refluxed solutions showed a significant decrease in the frequency of these smaller particles, which assembled to larger sized NFs (Figures 3d and 3e, respectively). The histogram evaluated from the TEM studies of the 6 h refluxed sample (see inset of Figure 3f) shows NFs within the size range of ~60-110 nm, with an average size (<D>) of 80 nm. The size of the NFs did not increase significantly with increasing reflux time beyond 6 h, as reflected by the TEM micrograph of the 9 h refluxed solution (Figure 3e). The presence of Pt has been confirmed from the EDX spectrum recorded from the 6 h refluxed sample, and is presented in Figure 3f. The presence of Cl, C and O resulted from the precursor metal salt (H_2PtCl_6) and the PVP, whereas Cu (and also C) appeared from the carbon-coated Cu grid used for the TEM analysis.

The surface of these nearly spherical 3D NFs was rough (observed from the FESEM image; Figure 4). It is confirmed that these PVP-stabilized nano-structured flowers, formed after the aggregation of individual particles, as observed in the just-turned dark Pt-solution, were highly stable, retaining their morphology and size beyond 6 h of refluxing.

The high angle XRD pattern obtained for the Pt NFs formed after 6 h of refluxing (Figure 5) reveals peaks at 39.76, 46.24, 67.45 and 81.28° 2θ values, corresponding to the (111), (200), (220) and (311) planes of the face-centred cubic crystal lattice of Pt, respectively (JCPDS# 00-04-0802). The low angle XRD pattern (inset of Figure 5) of the aforementioned NFs reveals a peak at 1.4° and a prominent shoulder at 1.93° 2θ, corresponding to the d values of 6.3 and 4.5 nm, respectively. This indicates that the maximum probable centre-to-centre nearest-neighbour distances of the nanoparticles in the NFs are around 6.3 and 4.5 nm rather than any random aggregation [31,34].

To visualize the morphology of the NFs, a detailed TEM study of these NFs was undertaken and presented in Figures 6a-f. Figures 6a and 6b (magnified) of the NFs show some ordered arrangement of the NPs within the NFs, with a uniform centre-to-centre nearest-neighbour distance of ~4.2 nm, which is consistent with the FFT of the NFs shown in the inset of Figure 6a as well as the d-value (~4.5 nm) obtained from the low angle XRD pattern. The center-to-center NPs' repeatation distance corresponding to the XRD peak at the d-value of 6.3 nm could not be observed in the TEM image. This may be due to the restricted tilting of viewing axes in TEM analysis. The selected area electron diffraction (SAED) pattern shown in Figure 6c confirms the crystalline nature of the Pt NFs, which is consistent with the high angle XRD results. The HRTEM image (shown in Figures 6d-e), as well as the FFT pattern (represented in Figure 6f), show lattice fringes corresponding to the (111), plane confirming the lattice orientations of the flowers along the (111) plane throughout the flowers. Thus, it is evident that the growth of the Pt NPs is not random; actually, the generated individual NPs of size ~4 nm (see Figure 3b)

act as seeds onto which the branches grow epitaxially to form ordered 3D flowers [10].

The role of the PVP during the growth of NPs can only be understood if we clarify the interaction of the PVP molecules with the metal NP surface. The protective effect of PVP in principle arises from the lone pair of electrons residing on the nitrogen and carbonyl oxygen atoms of PVP, which can be donated to the two sp hybrid orbitals of the metal ions to form complex ions [35,36] and it has been proved that this bonding between the PVP and the metal remains even when the metal ions are reduced [35]. Several research groups have investigated the protective mechanism of PVP over the past two decades [26-29, 35,36]. Some groups have claimed the presence of an interaction of both carbonyl oxygen and nitrogen atoms with the metal [28,29], whereas others established the existence of an interaction only through carbonyl oxygen atoms [36]. In a strongly acidic medium (pH ~2.5), PVP exists in cationic form and the bonding with Pt NPs becomes labile, while at elevated temperatures it becomes more labile and the metallic bond formation (between Pt metals) becomes more energetically favourable to the growth of the NPs into a flower shape. It is also evident that the epitaxial growth occurs along the <111> plane (evident from the HRTEM images; see Figures 3d and 3e), which is energetically favourable and, thus, the possibility of random growth has been ruled out.

It is therefore suggested that initially PVP is complexed with Pt ions, which is subsequently reduced by nascent hydrogen (see Eq. 1), and thereafter PVP stabilized Pt NPs nucleate to relatively larger NPs of size ~3-5 nm, following which these nuclei act as seeds for further growth during refluxing at 85 °C, as shown in scheme 1. It is observed that with increasing refluxing time, the size of the assembled particles increased and finally stabilized within the size range of ~60-110 nm.

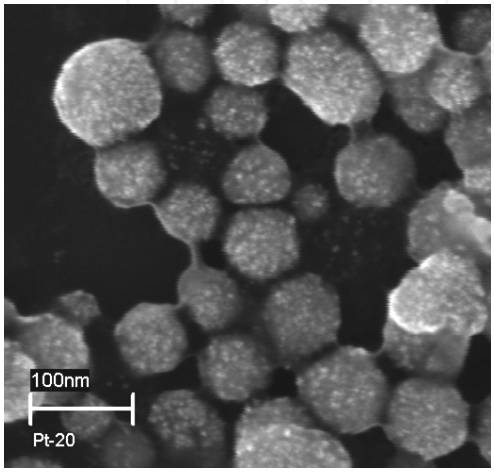

Figure 4. FESEM image of the Pt NFs obtained after refluxing for 6 h at 85 °C.

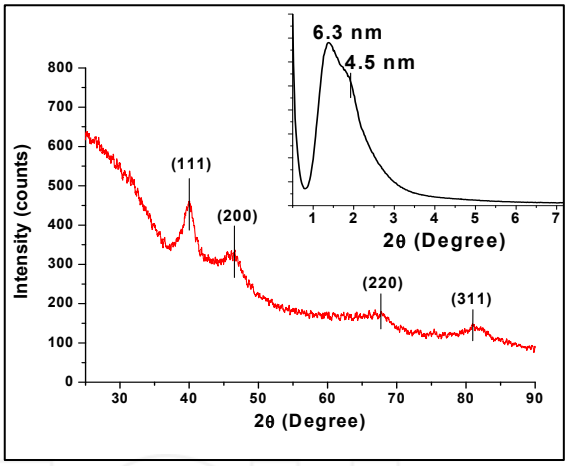

Figure 5. High and low (inset) angle X-ray diffraction patterns of the Pt-NFs. For this purpose, a 6 h refluxed solution was drop-casted onto a glass substrate, dried at 60 °C and analysed.

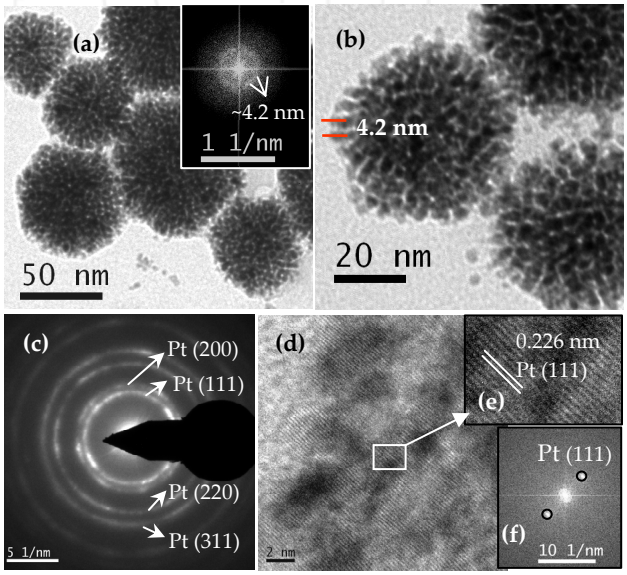

Figure 6. (a,b) TEM images of the Pt-NFs after 6h refluxing at different magnifications showing the ordered arrangement of the NFs. The FFT pattern obtained from the NFs is shown in the inset; (c) The SAED pattern obtained from a; (d,e) A high-resolution TEM image of a single NF depicting lattice fringes; and (f) The FFT pattern obtained from the HR image.

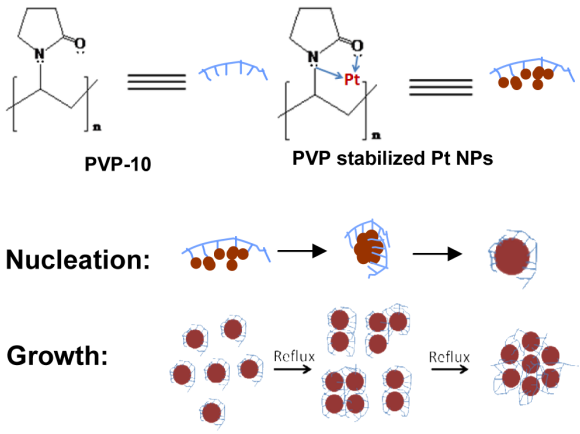

Scheme 1. Schematic illustration of formation and shape evolution of Pt nanoflowers.

4. Conclusions

In summary, we have demonstrated a facile and scalable approach towards the synthesis of ordered 3D Pt NFs by the ethanol reduction method at 85 °C in the presence of the capping agent PVP-10. The role of pH as well as the chain length of the PVP is crucial for the interaction of the PVP with NPs. The controlled reaction conditions lead to the generation and growth of nanoflower-shaped particles of Pt with an ordered structure. Due to this unique morphology, these Pt NFs could show very high electrocatalytic activity in DMFCs and catalytic activities in C-C coupling reactions.

5. Acknowledgement

The authors thank DST and CSIR, India for financial support.

6. References

[1] Wang Y, Shah N and Huffman G.P (2004) Pure hydrogen production by partial dehydrogenation of cyclohexane and methylcyclohexane over nanotube-supported Pt and Pd catalysts. Energy & Fuels 18: 1429–1433.

[2] Fukuoka A, Kimura J, Oshio T, Sakamoto Y and Ichikawa M (2007) Preferential oxidation of carbon monoxide catalyzed by platinum nanoparticles in mesoporous silica. J. Am. Chem. Soc. 129: 10120–10125.

[3] Li W, Liang C, Zhou W, Qiu J, Zhou Z, Sun G and Xin Q (2003) Preparation and characterization of multiwalled carbon nanotube-supported platinum for cathode catalysts of direct methanol fuel cells. J. Phys. Chem. B 107: 6292–6299.

[4] Dandapat A, Jana D and De G (2009) Synthesis of thick mesoporous γ-alumina films, loading of pt nanoparticles, and use of the composite film as a reusable catalyst. ACS Appl. Mater. Interfaces 1: 833–840.

[5] Sheng B, Hu L, Yu T, Cao X and Gu H (2012) Highly-dispersed ultrafine Pt nanoparticles on graphene as effective hydrogenation catalysts. RSC Adv. 2: 5520–5523.

[6] Dehouche F, Archirel P, Remita H, Brodie-Linder N and Traverse A (2012) Alcohol to water catalyzed by Pt nanoparticles: an experimental and computational approach. RSC Adv. 2: 6686–6694.

[7] Wang C, Daimon H, Onodera T, Koda T, Sun S and (2008) A general approach to the size- and shape-controlled synthesis of platinum nanoparticles and their catalytic reduction of oxygen. Angew. Chem. Int. Ed., 47: 3588–3591.

[8] Bratlie K.M, Lee H, Komvopoulos K, Yang P and Somorjai G.A (2007) Platinum nanoparticle shape effects on benzene hydrogenation selectivity. Nano Lett. 7: 3097–3101.

[9] Long N.V, Thi C.M, Nogami M and Ohtaki M (2012) Novel issues of morphology, size, and structure of Pt nanoparticles in chemical engineering: surface attachment, aggregation or agglomeration, assembly, and structural changes. New J. Chem. 36: 1320–1334.

[10] Mohanty A, Garg N and Jin R (2010) A universal approach to the synthesis of noble metal nanodendrites and their catalytic properties. Angew. Chem. Int. Ed. 49: 4962–4966.

[11] Liang H-P, Zhang H-M, Hu J-S., Guo Y-G, Wan L-J and Bai C-L (2004) Pt hollow nanospheres: facile synthesis and enhanced electrocatalysts. Angew. Chem. Int. Ed 3: 1540–1543.

[12] Li Y, Xian H and Zhou Y (2011) Formation of platinum nanoflowers on 3–aminopropyltriethoxysilane monolayer: growth mechanism and electrocatalysis. Appl. Catal. A: Gen. 401: 226–232.

[13] Tiwari J.N, Pan F and Lin K (2009) Facile approach to the synthesis of 3D platinum nanoflowers and their electrochemical characteristics. New J. Chem. 33: 1482–1485.

[14] Chen X, Su B, Wu G, Yang C J, Zhuang Z, Wangab X and Chen X (2012) Platinum nanoflowers supported on graphene oxide nanosheets: their green synthesis, growth mechanism, and advanced electrocatalytic properties for methanol oxidation. J. Mater. Chem. 22: 11284–11289.

[15] Ataee-Esfahani H, Nemoto Y, Wang L and Yamauchi Y (2011) Rational synthesis of Pt spheres with hollow interior and nanosponge shell using silica particles as template. Chem. Commun. 47: 3885–3887.

[16] Yamauchi Y, Ohsuna T and Kuroda K (2007) Synthesis and structural characterization of a highly ordered mesoporous Pt–Ru alloy via "evaporation-mediated direct templating". Chem. Mater. 19: 1335–1342.

[17] Wang H, Jeong H.Y, Imura M, Wang L, Radhakrishnan L, Fujita N, Castle T, Terasaki O and Yamauchi Y (2011) Shape- and size-controlled synthesis in hard templates: sophisticated chemical reduction for mesoporous monocrystalline platinum nanoparticles. J. Am. Chem. Soc. 133: 14526–14529.

[18] Chen J, Herricks T, Geissler M and Xia Y (2004) Single-crystal nanowires of platinum can be synthesized by controlling the reaction rate of a polyol process. J. Am. Chem. Soc. 126: 10854–10855.

[19] Ren J and Tilley R.D (2007) Shape-controlled growth of platinum nanoparticles. Small 3: 1508–1512.

[20] Sun S, Yang D, Villers D, Zhang G, Sacher E and Dodelet (2008) Template- and surfactant-free room temperature synthesis of self-assembled 3D pt nanoflowers from single-crystal nanowires. Adv. Mater. 20: 571–574.

[21] Kawasaki H, Yao T, Suganuma T, Okumura K, Iwaki Y, Yonezawa T, Kikuchi T and Arakawa R (2010) Platinum nanoflowers on scratched silicon by galvanic displacement for an effective SALDI substrate. Chem. Eur. J. 16: 10832–10843.

[22] Yamauchi Y and Kuroda K (2006) Fabrication of a Pt film with a well-defined hierarchical pore system via "solvent-evaporation-mediated direct physical casting". Electrochem. Commun. 8: 1677–1682.
[23] Yin J, Wang J, Li M, Jin C and Zhang T (2012) Iodine ions mediated formation of monomorphic single-crystalline platinum nanoflowers. Chem. Mater. 24: 2645−2654.
[24] Yang W, Wang Y, Li J and Yang X (2010) Polymer wrapping technique: an effective route to prepare Pt nanoflower/carbon nanotube hybrids and application in oxygen reduction. Energy Environ. Sci. 3: 144–149.
[25] Chen X, Su B, Wu G, Yang C J, Zhuang Z, Wang X and Chen X (2012) Platinum nanoflowers supported on graphene oxide nanosheets: their green synthesis, growth mechanism, and advanced electrocatalytic properties for methanol oxidation. J. Mater. Chem. 22: 11284–11289.
[26] Teranishi T, Hosoe M, Tanaka T and Miyake M (1999) Size control of monodispersed Pt nanoparticles and their 2D organization by electrophoretic deposition. J. Phys. Chem. B 103: 3818–3827.
[27] Narayanan R and El-Sayed M.A (2003) Effect of catalytic activity on the metallic nanoparticle size distribution: electron-transfer reaction between $Fe(CN)_6$ and thiosulfate ions catalyzed by PVP−platinum nanoparticles. J. Phys. Chem. B 107: 12416–12424.
[28] Zhang Z, Zhao B and Hu L (1996) PVP protective mechanism of ultrafine silver powder synthesized by chemical reduction processes. J. Solid State Chem. 121: 105–110.
[29] Jana D and De G (2011) Spontaneous generation and shape conversion of silver nanoparticles in alumina sol, and shaped silver nanoparticle incorporated alumina films. J. Mater. Chem. 21: 6072–6078.
[30] Borodko Y, Habas S.E, Koebel M, Yang P, Frei H and Somorjai G.A (2006) Probing the interaction of poly(vinylpyrrolidone) with platinum nanocrystals by UV−Raman and FTIR. J. Phys. Chem. B 110: 23052–23059.
[31] Whetten R.L, Khoury J.T, Alvarez M.M, Murthy S, Vezmar I, Wang Z.L, Stephens P.W, Cleveland C.L, Luedtke W.D and Landman U (1996) Nanocrystal gold molecules. Adv. Mater. 8: 428–433.
[32] Umar A.A and Oyama M (2006) Formation of gold nanoplates on indium tin oxide surface: two-dimensional crystal growth from gold nanoseed particles in the presence of poly(vinylpyrrolidone). Cryst. Growth Design 6: 818–821.
[33] Lim B, Jiang M, Tao J, Camargo P.H.C, Zhu Y and Xia Y (2009) Shape-controlled synthesis of Pd nanocrystals in aqueous solutions. Adv. Funct. Mater. 19: 189–200.
[34] Sarathy K.V, Raina G, Yadav R.T, Kulkarni G .U and Rao C.N.R (1997) Thiol-derivatised nanocrystalline arrays of gold, silver and platinum. J. Phys. Chem. B 101: 9876-9880.
[35] Pastoriza-Santos I and Liz-Marzan L.M (2009) N,N-Dimethylformamide as a reaction medium for metal nanoparticle synthesis. Adv. Funct. Mater. 19: 679–688
[36] Elechiguerra J.L, Larios-Lopez L, Liu C, Garcia-Gutierrez D, Camacho-Bragado A and Yacaman M (2005) Corrosion at the nanoscale: the case of silver nanowires and nanoparticles. Chem. Mater. 17: 6042–6052.